Magnetic and structural properties of Gd-implanted zinc-blende GaN

F.-Y. Lo,[a)] A. Melnikov, D. Reuter, and A. D. Wieck
Lehrstuhl für Angewandte Festkörperphysik, Ruhr-Universität Bochum, Universitätsstr. 150,
D-44780 Bochum, Germany

V. Ney, T. Kammermeier, and A. Ney
Experimentalphysik, Universität Duisburg-Essen, Lotharstr. 1, D-47057 Duisburg, Germany

J. Schörmann, S. Potthast, D. J. As, and K. Lischka
Department of Physics, Universität Paderborn, Warburger Str. 100, D-33098 Paderborn, Germany

Zinc-blende GaN layers grown by molecular beam epitaxy were uniformly focused-ion-beam implanted with 300 keV Gd^{3+} ions for doses ranging from 1×10^{12} to 1×10^{15} cm^{-2}, and their structural and magnetic properties were studied. The implanted samples were not subjected to any annealing treatment. Only Gd incorporation into zinc-blende GaN was observed by x-ray diffraction. Magnetic investigations using superconducting quantum interference device magnetometry reveal a (super)paramagneticlike behavior with an ordering temperature around 60 K for the sample with the highest implantation dose. Our experimental studies indicate that the spontaneous electric polarization in wurtzite GaN is the crucial mechanism for its ferromagneticlike behavior upon Gd doping. © *2007 American Institute of Physics*. [DOI: 10.1063/1.2753113]

The strong interest to study the incorporation of rare-earth (RE) elements into GaN is mainly driven by the potential for electronic and optoelectronic applications; for example, to develop blue, green, and red light emitting devices.[1,2] RE elements also have a strong atomic magnetic moment, so that the RE-doped GaN has an ample potential for the applications in spintronics, as well. Ferromagnetism with an ordering temperature T_c above room temperature was recently reported for very dilute Gd-doped wurtzite (WZ) GaN incorporated both by molecular beam epitaxy[3] (MBE) and by focused-ion-beam (FIB) implantation.[4] The ferromagnetic behavior was present in the aforementioned works for the Gd concentration as low as 1×10^{16} cm^{-3}, and moreover, at 2 K, the effective magnetic moment per Gd atom p_{eff}, ($p_{eff}=M(50$ kOe$)/n_{Gd}$), was found to be as high as $4000\mu_B$ for MBE doping and $1 \times 10^5 \mu_B$ for FIB implantation. These values are huge compared to the atomic magnetic moment of Gd, $8\mu_B$. Therefore, it was postulated that defects contribute to the interaction between Gd atoms in the WZ GaN matrix, but the microscopic origin of these effects is not yet understood, especially since all these samples are highly resistive.

Zinc-blende (ZB) GaN having a cubic symmetry has more isotropic properties; especially, the spontaneous electric polarization known from the WZ GaN is not found in ZB GaN, which results in smaller effective masses, higher carrier mobility, and doping efficiency.[5] Therefore, ZB GaN is expected to be more suitable than WZ GaN for certain electronic device applications. Theoretical work on ZB $Ga_{1-x}Gd_xN$ based on *ab initio* band calculations and symmetry arguments suggests that the ferromagnetic phase is only stable when donor atoms are introduced into the material.[6] Thus, *n*-type Gd-doped ZB GaN seems to be a better candidate for spintronic application than *n*-type or even resistive Gd-doped WZ GaN.

In this letter, we report the structural and the magnetic properties of *n*-type ZB GaN films doped with Gd by FIB implantation at different doses which are compared to Refs. 4 and 6. Our study shows that in the implantation dose range between 1×10^{12} and 1×10^{15} cm^{-2}, the Gd atoms were incorporated into the ZB GaN, and the crystal structure keeps its cubic symmetry. The magnetic ordering was observed only for the highest implantation dose and further restricted to low temperatures with an ordering temperature around 60 K.

A nonintentionally doped 700 nm thick ZB GaN layer was grown by MBE on a 3*C*-SiC (001) substrate at 720 °C.[7] Under this growth condition, the ZB GaN is *n* type, and the impurity concentration is typically around 1×10^{18} cm^{-3} as determined by capacitance voltage spectroscopy on similar samples. The sample was then cut into four pieces of the same size (5×5 mm^2) and labeled numerically. Sample 4 was kept unimplanted as a reference, and the others were implanted with Gd^{3+} ions by using a 100 kV FIB implanter (EIKO-100). The implantations were carried out at room temperature with a constant ion energy of 300 keV. The implantation doses for samples 1 and 2 were 1×10^{13} and 1×10^{15} cm^{-2}, respectively. Sample 3 was first implanted with a dose of 1×10^{12} cm^{-2}, and after magnetic measurements, it was again implanted with a dose of 1×10^{14} cm^{-2}. All implanted samples were not subjected to any annealing treatment. The projected range of the Gd ion in the samples is 100 nm, which was calculated using the SRIM program.[8] The average Gd concentration in the sample was estimated by integrating the ion distribution over the implantation profile and dividing by the projected range, which yields the corresponding Gd concentrations, from 1×10^{17}, 1×10^{18}, and 1×10^{19} to 1×10^{20} cm^{-3} (equivalent to $x=0.0023$). The change in the resistance of the thin implanted ZB GaN layer due to the implantation cannot be determined due to the fact that both the unimplanted ZB GaN layer and the highly conducting 3*C*-SiC substrate contribute in the electrical measurements. From measurements on GaN/Al_xGa_{1-x}N het-
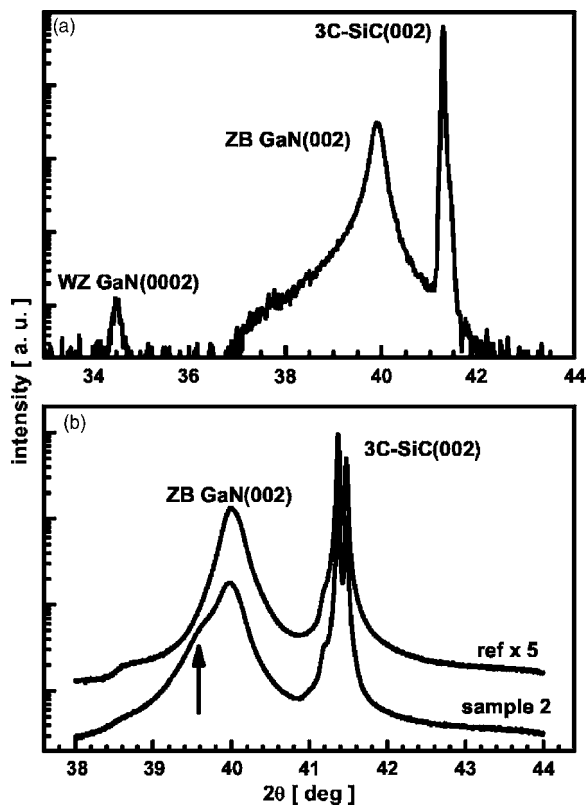
a)Electronic mail: fang-yuh.lo@rub.de

FIG. 1. X-ray diffraction ω-2θ scan of (a) the as-grown sample and (b) the Gd-implanted sample 2 with the concentration, 1×10^{20} cm^{-3}, and the reference sample. The arrow shows the Gd-related broadening.

FIG. 2. Magnetization loops obtained from samples 2, 3, and 4 at (a) T=5 K and (b) T=300 K. The unimplanted and Gd-implanted curves are in solid and open symbols, respectively. The inset shows the loop corrected for the diamagnetic background for sample 2 at T=5 K after implantation.

erostructures (wurtzite structure), we would suspect an increase of the resistance but at least at the lowest dose investigated, the layer should remain well conducting.

The structural properties were investigated by x-ray diffraction (XRD) recorded with a Philips X'Pert MRD diffractometer after the crystal growth and FIB implantations. The magnetic properties were measured with a Quantum Design superconducting quantum interference device (SQUID) magnetometer. For all the SQUID measurements, the magnetic field was applied parallel to the sample surface. The magnetization loops were recorded at 5 and 300 K for magnetic fields between ±50 kOe. The temperature dependence of the magnetization was investigated by field-cooled (FC), zero-FC (ZFC), and temperature-dependent remanent (TR) magnetization curves measured between 2 and 300 K. The samples were cooled either under a saturation magnetic field of 50 kOe (FC) or zero field (ZFC), and then the magnetization was measured at a magnetic field of 100 Oe while warming up the samples. For the TR curves, a 30 kOe magnetic field was applied to the samples prior to the cooling and warming-up processes, and then the samples were cooled down or warmed up in zero field while the remanence was measured.

Figure 1 shows the x-ray ω-2θ scan, which was performed in the double axis configuration right after the film growth (a) and after FIB implantation (b). Though the diffraction pattern shows a clear ZB GaN (002) peak at 39.9° in 2θ, there exists the WZ GaN (0002) peak at 34.5° in 2θ. From the ratio of the integrated intensity between both peaks, more than 99.5% of the GaN layer was found in the ZB phase. After Gd implantation, only the ZB GaN (002) peak features the Gd-related broadening known from WZ
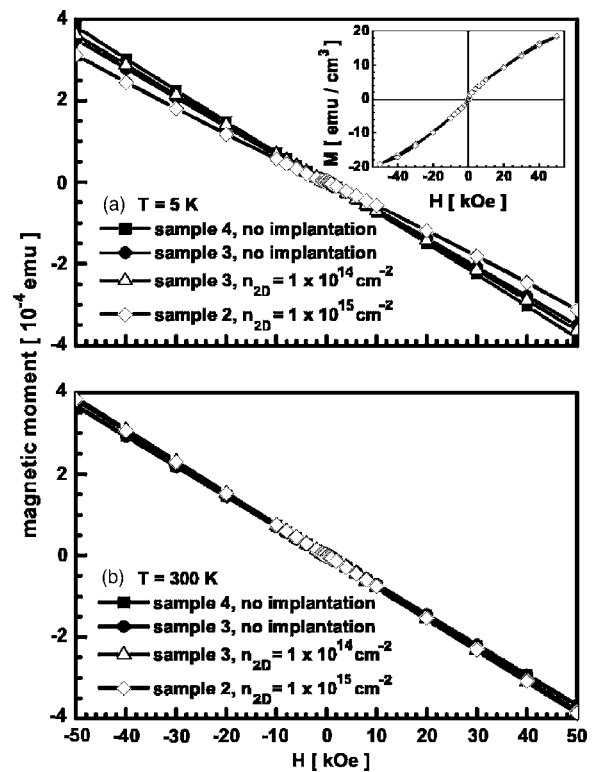
Gd-implanted GaN,[4] which indicates that the nucleation of the WZ phase occurred at the interface between the GaN and the 3C-SiC substrate during the initial growth process, and it did not extend to the sample surface.

All samples including the unimplanted reference piece 4 were subjected to magnetic measurements before Gd implantation. Figure 2(a) shows the as-measured hysteresis loops at 5 K for sample 4, sample 3 before and after Gd implantation (dose of 1×10^{14} cm^{-2}), and Gd-implanted sample 2 (dose of 1×10^{15} cm^{-2}). The reference sample shows the expected diamagnetic behavior between ±50 kOe. The hysteresis loops of the three lower Gd concentrations show no difference from the reference curves, and only sample 2 implanted with the highest dose shows a distinguishable but very small additional signal. After the diamagnetic background was subtracted, the magnetization loop of sample 2 shows only a weak hysteretic behavior at 5 K and, therefore, the magnetization is not saturated up to the highest field of 50 kOe indicating a strong paramagnetic contribution to the overall signal [Fig. 2(a) inset]. The total magnetization of the sample is around 18.5 emu/cm^3 at 50 kOe, and the p_{eff} is around $20\mu_B$, which is roughly one half of that observed at 2 K in Gd-implanted epitaxially grown WZ GaN layers of the same dose.[4] For the as-measured hysteresis loops at 300 K, shown in Fig. 2(b), all the samples exhibit only a diamagnetic behavior between ±50 kOe which is in strong contrast with WZ GaN, where a clear magnetic hysteresis could be recorded up to room temperature for all implantation doses.[4]

All implanted samples but sample 2 show the same temperature-dependent behavior as the reference sample (sample 4). The comparison of FC and ZFC curves between samples 4 and 2 is depicted in Fig. 3(a), and the comparison
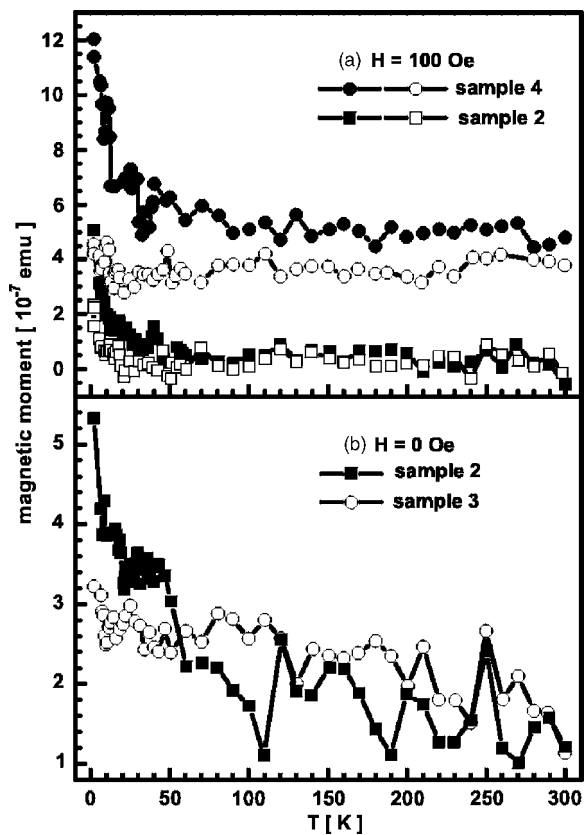
FIG. 3. Temperature dependence of the magnetizations at (a) field-cooled (solid symbols) and zero-field-cooled (open symbols) conditions at a magnetic field of 100 Oe, and (b) remanence during warming up processes.

of the TR curves between samples 3 and 2 is depicted in Figure 3(b). Qualitatively, FC and ZFC curves of the three lower Gd concentrations and the reference sample have only a strong temperature dependence of the magnetization below 10 K as well as the ZFC curve of sample 2, and this dependence is paramagneticlike. In addition to the paramagneticlike behavior, the FC curve of sample 2 has a weak temperature dependence between 10 and 60 K, indicative of a long-range magnetic ordering. The warming-up TR curves other than that of sample 2 have no magnetic signal beyond the small value recorded for the reference sample, which is presumably a fitting artifact from the SQUID. For sample 2, a very small finite remanence is visible up to about 60 K, having a weak temperature dependency, which means that a low temperature magnetically ordered phase may exist for the highest implantation dose up to about 60 K. Note that this temperature roughly coincides with the order temperature of rocksalt GdN, which is ferromagnetic up to about 60 K.[9] However, we have no indications of phase segregated GdN by means of XRD.

Although the magnetic ordering phase of sample 2 has the ferromagneticlike temperature dependence, the rounded magnetization loop together with the FC/ZFC behavior suggests that this sample is more superparamagneticlike rather than ferromagnetic. One reason that none of the samples show no or—in the case of the highest dose—only a low temperature ferromagnetic ordering can be attributed to the low Gd and donorlike impurity concentrations, which are orders of magnitudes smaller than the theoretical calculation. The highly localized character of the f orbitals of Gd leading

only to a weak electron-mediated interaction may account for that. Furthermore, the increase in the resistivity and the decrease in the electron concentration of the ZB GaN after Gd implantation could also be another reason. In other words, to have ZB $Ga_{1-x}Gd_xN$ having RT ferromagnetism, higher Gd and electron concentrations are needed.

Comparing the results for ZB GaN presented here to the ones on WZ GaN in Ref. 4, there are two major differences: (i) RT ferromagnetic ordering and the colossal magnetic moment at very low Gd concentration (1×10^{16} cm^{-3}) for WZ $Ga_{1-x}Gd_xN$ and (ii) their highly resistive property. The former indicates that there exists a very strong long-range interaction between the Gd atoms and/or between Gd atoms and defects in the WZ GaN matrix. The latter suggests that (a) there is no free-carrier-mediated interaction as in our n-type ZB $Ga_{1-x}Gd_xN$—this is even less favorable of ferromagnetic ordering, and (b) all the Gd–Gd and the Gd-defect interactions are highly localized. As pointed out by Svane *et al.*, rare-earth dopants unlikely by themselves induce the RT ferromagnetism and the colossal magnetic moment. Thus, the Gd has to interact via certain defects, either native or external.[10] In the view of our present experiments it seems imperative to suggest that the spontaneous electric polarization—the only long-range interaction in the undoped WZ GaN—seems to be essential to yield the long-range magnetic order in WZ GaN.

In conclusion, our study found a magnetic ordering in n-type nonintentionally doped zinc-blende $Ga_{1-x}Gd_xN$ only for a Gd concentration of 1×10^{20} cm^{-3}. The magnetic order is restricted to temperatures below 60 K, and FC/ZFC measurements indicate a blockinglike behavior rather than ferromagnetism. Comparison between our results and those obtained from FIB Gd-implanted WZ GaN indicates that the spontaneous electric polarization in WZ GaN is the driving mechanism for the ferromagneticlike behavior in WZ $Ga_{1-x}Gd_xN$.

[1] Y. Q. Wang and A. J. Steckl, Appl. Phys. Lett. **82**, 502 (2003).
[2] K. Wang, R. W. Martin, K. P. O'Donnell, V. Katchkanov, E. Nogales, K. Lorenz, E. Alves, S. Ruffenach, and O. Briot, Appl. Phys. Lett. **87**, 112107 (2005).
[3] S. Dhar, O. Brandt, M. Ramsteiner, V. F. Sapega, and K. H. Ploog, Phys. Rev. Lett. **94**, 037205 (2005).
[4] S. Dhar, T. Kammermeier, A. Ney, L. Pérez, K. H. Ploog, A. Melnikov, and A. D. Wieck, Appl. Phys. Lett. **89**, 062503 (2006).
[5] L. E. Ramos, J. Furthmüller, J. R. Leite, L. M. R. Scolfaro, and F. Bechstedt, Phys. Rev. B **68**, 085209 (2003).
[6] G. M. Dalpian and S.-H. Wei, Phys. Rev. B **72**, 115201 (2005).
[7] J. Schörmann, S. Potthast, D. J. As, and K. Lischka, Appl. Phys. Lett. **90**, 041918 (2007).
[8] J. F. Ziegler and J. P. Biersack, http://www.srim.org/
[9] F. Leuenberger, A. Parge, W. Felsch, F. Baudelet, C. Giorgetti, E. Dartyge, and F. Wilhelm, Phys. Rev. B **73**, 214430 (2006).
[10] A. Svane, N. E. Christensen, L. Petit, Z. Szotek, and W. M. Temmerman, Phys. Rev. B **74**, 165204 (2006).